ARCH DAM OPTIMIZATION CONSIDERING FLUID-STRUCTURE INTERACTION WITH FREQUENCY CONSTRAINTS USING ARTIFICIAL INTELLIGENCE METHODS

J. Salajegheh[1] , E. Salajegheh[2] , S.M. Seyedpoor[3] and S. Gholizadeh[3]

[1] *Dr, Dept. of Civil Engineering, University of Kerman, Kerman. Iran*
[2] *Professor, Dept. of Civil Engineering, University of Kerman, Kerman. Iran*
[3] *Ph.D. Student, Dept. of Civil Engineering, University of Kerman, Kerman. Iran*
Email: eysasala@mail.uk.ac.ir

ABSTRACT:
An efficient method is proposed to find optimal design of arch dams on the basis of constrained natural frequencies utilizing continuous evolutionary algorithm. To extract natural frequencies of arch dam considering fluid-structure interaction, it is necessary to solve the unsymmetrical damped eigenproblem. This means that the process of natural frequencies extraction may impose much computational effort. This deficiency can be resonated when a grate number of structural analyses are needed during the optimization process. In order to reduce the computational cost of the optimization problem, the natural frequencies of arch dam are predicted by properly trained back propagation (BP) and wavelet back propagation (WBP) neural networks. The presented WBP network appears better performance generality than BP network. The numerical results reveal the computational advantages of the proposed methods for optimal design of arch dams.

KEYWORDS: arch dam, natural frequency, optimum design, wavelet theory, neural networks.

1. INTRODUCTION

It is obvious that the natural frequencies are important parameters which affect the dynamic behavior of arch dams. By imposing some constraints on the natural frequencies, the dynamic behavior of arch dam may be improved and the eventual resonance phenomenon during earthquake can be also eliminated. This aim can be reliably implemented by employing optimization techniques [1]. In the last years, some progress has been made in optimal design of arch dams. Almost all of them have used conventional methods for analysis approximation and optimization [2-4]. The main disadvantage of these methods is to require calculating function derivatives and may also trap into local optima. Evolutionary algorithms are computationally efficient in comparison with gradient based methods [5-8]. In this study, an efficient method is presented to optimize double curvature arch dams considering fluid-structure interaction with constrained natural frequencies utilizing continuous evolutionary algorithm. The evolutionary algorithm employed here is based on virtual sub population (VSP) method [9]. The concrete volume of dam body is selected as objective function. The design variables are principal geometric parameters of arch dam and the design constraints are taken as limits on natural frequencies as well as some geometric requirements.

The nature of the numerical optimization methods is such that great number of function evaluations is required to achieve the optimal solution. In particular, to extract the natural frequencies of the arch dam-water system, each function evaluation requires an unsymmetrical damped eigenproblem analysis. Moreover, the stochastic nature of evolutionary search techniques makes the convergence of the process slow. Therefore, complete optimization of arch dams for frequency constraints requires disproportionate computer work. In order to accelerate the optimization process and reduce the computational effort, the natural frequencies of arch dams are predicted using properly trained neural networks instead of direct evaluation. Back propagation (BP) and wavelet back propagation (WBP) neural networks are employed for this meaning [10-13].

The numerical results reveal the high performance of the suggested methods for optimum design of arch dams. It is found that the optimum design obtained by VSP using the WBP network is much better than the others.

2. GEOMETRICAL MODEL OF ARCH DAM

2.1. Shape of Central Vertical Section

For the central vertical section of double-curvature arch dam one polynomial of *n*th order can be used to determine the curve of upstream boundary and another polynomial can be used to determine the thickness [2, 3]. In this study, for the curve of upstream face a polynomial of *2*nd order is considered as:

$$y(z) = b(z) = -s\,z + s\,z^2 / (2\,\beta\,h) \tag{2.1}$$

where h and s are the height of the dam and the slope of at crest, respectively. The point where the slope of the upstream face equals to zero is $z=\beta\,h$.
By dividing the height of dam into n segments, the thickness of central vertical section can be expressed as:

$$tc(z) = \sum_{i=1}^{n+1} f_i(z)\,tc_i \tag{2.2}$$

in which t_{c_i} is the thickness of the central vertical section at ith level. Also, in the above relation $f_i(z)$ is Lagrange interpolation function associated with ith level and can be defined as:

$$f_i(z) = \frac{\prod_{k=1}^{n+1}(z - z_k)}{\prod_{k=1}^{n+1}(z_i - z_k)} \qquad \text{k} \neq \text{i} \tag{2.3}$$

where z_i denotes the z coordinate of ith level in the central vertical section.

2.2. Shape of Horizontal Section

For the purpose of symmetrical canyon and arch thickening from crown to abutment, the shape of the horizontal section of a parabolic dam is determined by the following two parabolic surfaces [3]:

At the upstream face of dam:
$$y_{\text{u}}(x,z) = \frac{1}{2\,r_u(z)}\,x^2 + b(z) \tag{2.4}$$

At the downstream face of dam:
$$y_{\text{d}}(x,z) = \frac{1}{2\,r_d(z)}\,x^2 + b(z) + t_c(z) \tag{2.5}$$

where r_u and r_d are radii of curvature correspond to upstream and downstream curves, respectively and the functions of nth order with respect to z can be used for those radii.

$$r_u(z) = \sum_{i=1}^{n+1} f_i(z)\,r_{ui} \tag{2.6}$$

$$r_d(z) = \sum_{i=1}^{n+1} f_i(z)\,r_{di} \tag{2.7}$$

where r_{u_i} and r_{d_i} are the values of r_u and r_d at ith level , respectively.

3. FINITE ELEMENT MODEL OF ARCH DAM-RESERVOIR SYSTEM

In fluid-structure problems the discretized structural dynamic equation and fluid equation need to be considered simultaneously. The governing equation in the fluid domain is acoustic wave equation as follows [14-17]:

$$\frac{1}{\mathrm{c}^2}\frac{\partial^2 p}{\partial^2 t} - \nabla^{\mathrm{T}}\nabla\, p = 0 \tag{3.1}$$

where c is speed of pressure wave, $p=p(x, y, z, t)$ is acoustic pressure and t is time. Furthermore, $\nabla^T = \{\partial/\partial x^2\ \partial/\partial y^2\ \partial/\partial z^2\}$ in the above relation is Laplas operator. Some boundary conditions are imposed on Eq. 3.1 from which the following boundary condition must be considered on the interface:

$$\boldsymbol{n}^{\mathrm{T}}\nabla\, p = -\rho_{\mathrm{w}}\, \boldsymbol{n}^{\mathrm{T}}\frac{\partial^2 \boldsymbol{u}}{\partial t^2} \tag{3.2}$$

where $\boldsymbol{n}$ is a unit normal vector to the interface, $\boldsymbol{u}$ is displacement vector of the structure at the interface and ρ_w is mass density of water. At the fluid boundaries, a condition is required to account for the dissipation of energy due to damping as:

$$\frac{\partial p}{\partial \boldsymbol{n}} = -\frac{\kappa}{\mathrm{c}}\frac{\partial p}{\partial t} \tag{3.3}$$

where $0 \le \kappa \le 1$ is boundary absorption coefficient.
At the free surface, when the surface wave is neglected, boundary condition is easily defined as:

$$\boldsymbol{M}_f\ddot{\boldsymbol{p}}_{\mathrm{e}} + \boldsymbol{C}_f\dot{\boldsymbol{p}}_{\mathrm{e}} + \boldsymbol{K}_f\boldsymbol{p}_{\mathrm{e}} + \rho_{\mathrm{w}}\boldsymbol{Q}^{\mathrm{T}}(\ddot{\boldsymbol{u}}_{\mathrm{e}} + \ddot{\boldsymbol{u}}_{\mathrm{g}}) = 0 \tag{3.4}$$

Eqns. 3.1 to 3.4 can be discretized to get the matrix form of wave equation as:

$$p = 0 \tag{3.5}$$

where $\boldsymbol{M}_{\mathrm{f}}$, $\boldsymbol{C}_{\mathrm{f}}$ and $\boldsymbol{K}_{\mathrm{f}}$ are fluid mass, damping and stiffness matrices, respectively and $\boldsymbol{p}_e$, $\ddot{\boldsymbol{u}}_e$ and $\ddot{\boldsymbol{u}}_g$ are nodal pressure, acceleration and ground acceleration vectors, respectively. Also, $\rho_w\boldsymbol{Q}^T$ in the above relation is often referred to as coupling matrix.
The discretized structural dynamics equation for ground motion can be formulated using the finite elements as:

$$\boldsymbol{M}_s\ddot{\boldsymbol{u}}_{\mathrm{e}} + \boldsymbol{C}_s\dot{\boldsymbol{u}}_{\mathrm{e}} + \boldsymbol{K}_s\boldsymbol{u}_{\mathrm{e}} = -\boldsymbol{M}_s\ddot{\boldsymbol{u}}_g + \boldsymbol{Q}\boldsymbol{p}_{\mathrm{e}} \tag{3.6}$$

where $\boldsymbol{M}_{\mathrm{s}}$, $\boldsymbol{C}_{\mathrm{s}}$ and $\boldsymbol{K}_{\mathrm{s}}$ are structural mass, damping and stiffness matrices, respectively and $\boldsymbol{u}_{\mathrm{e}}$ is nodal relative displacement vector. Also, $\boldsymbol{Qp}_{\mathrm{e}}$ term in Eqn. 3.6 represents nodal force vector associated with hydrodynamic pressure produced by reservoir.
Eqns. 3.5 and 3.6 describe the complete finite element discretized equations for the fluid-structure interaction problem and are written in assembled form as:

$$\begin{bmatrix} \boldsymbol{M}_s & 0 \\ \boldsymbol{M}_{fs} & \boldsymbol{M}_f \end{bmatrix}\begin{Bmatrix} \ddot{u}_e \\ \ddot{p}_e \end{Bmatrix} + \begin{bmatrix} \boldsymbol{C}_s & 0 \\ 0 & \boldsymbol{C}_f \end{bmatrix}\begin{Bmatrix} \dot{u}_e \\ \dot{p}_e \end{Bmatrix} + \begin{bmatrix} \boldsymbol{K}_s & \boldsymbol{K}_{fs} \\ 0 & \boldsymbol{K}_f \end{bmatrix}\begin{Bmatrix} u_e \\ p_e \end{Bmatrix} = \begin{Bmatrix} -\boldsymbol{M}_s\ddot{u}_g \\ -\boldsymbol{M}_{fs}\ddot{u}_g \end{Bmatrix} \tag{3.7}$$

where $\boldsymbol{M}_{fs} = \rho_{\mathrm{w}}\boldsymbol{Q}^T$ and $\boldsymbol{K}_{fs} = -\boldsymbol{Q}$.

Eqn. 3.7 can also be written alternatively in a more compact form:

$$\boldsymbol{M}\ddot{\boldsymbol{u}} + \boldsymbol{C}\dot{\boldsymbol{u}} + \boldsymbol{K}\boldsymbol{u} = F(t) \tag{3.8}$$

where ***M***, ***C*** and ***K*** are mass, damping and stiffness matrices of dam-reservoir system, respectively. Obviously, ***M*** and ***K*** are not symmetric matrices. Since the system damping matrix needs to be included in modal analysis, the eigenproblem becomes a quadratic eigenvalue problem as:

$$(\lambda_i^2 \boldsymbol{M} + \lambda_i \boldsymbol{C} + \boldsymbol{K})\boldsymbol{\varphi}_i = 0 \quad , \quad i = 1,\ldots,ndf \tag{3.9}$$

The above equation needs to be solved to get the complex eigenvalues λ_i given by:

$$\lambda_i = \sigma_i \pm \omega_i j \quad , \quad i = 1,\ldots,ndf \tag{3.10}$$

where σ_i and ω_i are real and imaginary part of the eigenvalue and $j=\sqrt{-1}$. In this case, natural frequency is calculated as:

$$fr_i = \frac{\sqrt{\sigma_i^2 + \omega_i^2}}{2\pi} \quad , \quad i = 1,\ldots,ndf \tag{3.11}$$

In the present study, the finite element model of double-curvature arch dam considering fluid-structure interaction is employed based on the mentioned theory and assumptions. The arch dam is treated as a 3D-linear structure. An eight-nodded solid element is utilized to mesh of the dam body. The reservoir is assumed to be uniform shape and eight-nodded fluid element is used to discretize the fluid medium and the interface of the fluid-structure interaction problem [16]. The element has four degrees of freedom per node: translations in the nodal x, y and z directions and pressure. The translations, however, are applicable only at nodes that are on the interface. In this study, interaction between dam and the foundation rock is not considered and it is assumed to be rigid to avoid the extra complexities that would otherwise arise. Interaction between the fluid and foundation rock is approximately considered thorough a damping boundary condition applied along the bottom and sides of the reservoir. The finite element model of arch dam-water system is depicted on Figure 1.

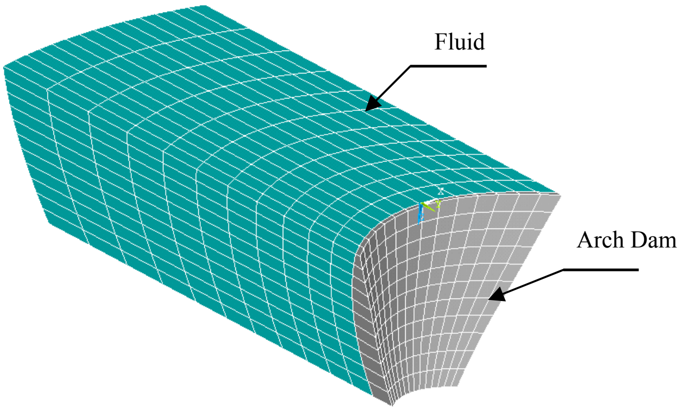

Figure 1 Finite element model of arch dam-water system

3.1. Verification of the FE Model

In order to assist in validating the finite element model with the employed assumptions an idealized symmetric model of Morrow Point arch dam which is located 263 km southwest of Denver, Colorado, is investigated. The properties of the dam in details can be found in Ref [14]. The first three natural frequencies of the symmetric mode of Morrow Point dam are determined from the frequency response function for the crest displacement and the results are compared with those of reported in the literature [18-20]. The natural frequencies from the literature and the finite element model are given in Table 3.1 It can be observed that a good conformity has been achieved between the results of present work with those of reported in the literature.

Table 3.1 Comparison of the natural frequencies from the literature with FE model

Symmetric mode	Natural frequencies (Hz)					
	From the literature				Present work	
	Tan and Chopra		Duran and Hall (FEA)	Duran and Hall (Experimental)	Empty reservoir	Full reservoir
	Empty reservoir	Full reservoir				
1	4.27	2.82	3.05	2.95	4.29	2.80
2	-	-	4.21	3.95	6.71	3.76
3	-	-	5.96	5.40	-	5.57

4. WAVELET BACK PROPAGATION NEURAL NETWORK

Recently, researchers have proven that the wavelet type of neural networks possess better performance generality in comparison with their conventional versions [1 ,11]. In wavelet networks, both the position and the dilation of the wavelets may be optimized besides the weights. In the present study, wavelet neural network is referred to network using wavelets as activation function of hidden layer neurons with the fixed position and the dilation. The daughter wavelets are generated from a single mother wavelet $h(t)$ by dilation and translation:

$$h_{j,k}(t) = \frac{1}{\sqrt{j}} h\left(\frac{t-k}{j}\right) \tag{4.1}$$

where $j > 0$ and k are the dilation and the translation factors, respectively [21].
Substituting of BP neurons activation function with some wavelet functions may improve its performance generality. To design wavelet back propagation (WBP) network the activation function of hidden layer of BP network is substituted with Mexican Hat (MexH) wavelet function [22]:

$$h_{\mathrm{MexH}}(t) = \left(\frac{2}{\sqrt{3}}\pi^{-0.25}\right)(1 - t^2)\, e^{-t^2/2} \tag{4.2}$$

This function is proportional to the second derivative function of the Gaussian probability density function. The daughter MexH wavelet is obtained by substituting Eqn. 4.2 into Eqn. 4.1:

$$h^{j,k}_{\mathrm{MexH}}(t) = \left(\frac{2}{\sqrt{3}}\pi^{-0.25}\right)\frac{1}{\sqrt{j}}\left(1 - \left(\frac{t-k}{j}\right)^2\right) e^{\left(-\left(\frac{t-k}{j}\right)^2\right)/2} \tag{4.3}$$

In this study, to design WBP network, the position and dilation of the MexH wavelets are fixed and only the network weights are optimized by Levenberg-Marquardt (LM) [23] algorithm. The best results are obtained by considering $j = 2$ and $k = 0$ in Eqn. 4.3.

5. ARCH DAM OPTIMIZATION

5.1. Mathematical Model and Optimization Variables

The optimization problem is formally stated as follows:

$$\begin{aligned} &\text{Minimize} \quad z(\boldsymbol{x}) \\ &\text{Subject to} \quad g_j(\boldsymbol{x}) \le 0\,,\ j = 1,\ldots,m \end{aligned} \tag{5.1}$$

where $\boldsymbol{x}$ is the design variable vector with n unknowns, $g_j,(j=1,\ldots m)$ are inequality constrains including the side constraints and $z(\boldsymbol{x})$ represents the objective function that should be minimized.

5.1.1. Design variables

The most effective parameters for creating the arch dam geometry were mentioned in section 2. These parameters can be adopted as design variables:

$$\boldsymbol{x}^{\mathrm{T}} = \{s \;\; \beta \;\; t_{c1} \ldots t_{c\,n+1} \;\;\; r_{u1} \ldots r_{u\,n+1} \;\;\; r_{d1} \ldots r_{d\,n+1}\} \tag{5.2}$$

where $\boldsymbol{x}$ vector may have $3n+5$ components involving shape parameters of arch dam.

5.1.2. Design constraints

Design constraints are divided into some groups including the behavior, geometric and stability constraints. The behavior constraints are limits on natural frequencies that may be defined as follows:

$$fr_k^l \le fr_k \le fr_k^u \;\Rightarrow \begin{cases} g_{bk}^l(\boldsymbol{x}) = 1 - \dfrac{fr_k}{fr_k^l} \le 0 \\ g_{bk}^u(\boldsymbol{x}) = \dfrac{fr_k}{fr_k^u} \text{-} 1 \le 0 \end{cases} \quad , \quad k = 1,2,\ldots,n_{\mathrm{fr}} \tag{5.3}$$

where fr_k , fr^l_k and fr^u_k are the kth natural frequency, lower and upper bounds on kth natural frequency, respectively. Also, n_{fr} is the number of natural frequencies that may be considered.
The most important geometric constrains are those that prevent from intersection of upstream and downstream face as:

$$r_{d\,i} \le r_{u\,i} \Rightarrow g_{gi}(\boldsymbol{x}) = \frac{r_{d\,i}}{r_{u\,i}} - 1 \le 0 \quad , \quad i = 1,\ldots,n+1 \tag{5.4}$$

where r_{di} and r_{ui} are radii of curvatures at the down and upstream faces of the dam in ith position in z direction. The geometric constrain that is applied for facile construction, is defined as:

$$s \le s_{all} \Rightarrow \mathrm{g_c}(\boldsymbol{x}) = \frac{s}{s_{all}} - 1 \le 0 \tag{5.5}$$

where s is the slope of overhang at the upstream face of dam and s_{all} is its allowable value. s_{all} is taken as 0.3. The constraints ensuring the sliding stability of the dam may be expressed as:

$$\varphi^{\mathrm{l}} \le \varphi_{\mathrm{i}} \le \varphi^{\mathrm{u}} \Rightarrow \begin{cases} g_{si}^u(\boldsymbol{x}) = \dfrac{\varphi_{\mathrm{i}}}{\varphi^{\mathrm{u}}} - 1 \le 0 \\ g_{si}^l(\boldsymbol{x}) = 1 - \dfrac{\varphi_{\mathrm{i}}}{\varphi^{\mathrm{l}}} \le 0 \end{cases} \quad , \quad \mathrm{i} = 1,\ldots,\mathrm{n}+1 \tag{5.6}$$

where φ_i is the ith central angle of arch dam and usually $90 \le \varphi_i \le 130$.

5.1.3. Objective function

In the present work, the concrete volume of arch dam body is considered as objective function that is determined by integrating of dam surfaces as:

$$w(\hat{\boldsymbol{x}}) = vol(\hat{\boldsymbol{x}}) = \iint_{Area} \left| y_d(x,z) - y_u(x,z) \right| \mathrm{d}\,x\,\mathrm{d}\,z \tag{5.7}$$

in which $vol(\hat{\boldsymbol{x}})$ is concrete volume of dam expressed in term of design variable vector and *Area* is an area produced by projecting of dam body on *xz* plane. In order to evaluate in this study, exterior penalty function method is employed to transform constrained dam optimization problem into unconstrained one as follows:

$$\mathrm{w}(\boldsymbol{x},\gamma_\mathrm{p}) = \mathrm{z}(\boldsymbol{x})[1+\gamma_\mathrm{p}\sum_{\mathrm{j=1}}^{\mathrm{m}}\max(\mathrm{g_j}(\boldsymbol{x}),0)^2] \tag{5.8}$$

in which $w(\boldsymbol{x})$ is pseudo objective function and γ_p is penalty multiplier.

6. MAIN STEPS OF ARCH DAM OPTIMIZATION

The main steps for the optimization of arch dams under frequency constraints by VSP employing BP and WBP are summarized as follows:

Data generation and neural networks training:

(a) Some arch dams considering their geometric parameters are selected randomly.
(b) Natural frequencies of the selected dams are evaluated by ANSYS [15].
(c) By using the geometric parameters of the generated dams as the inputs and the corresponding natural frequencies as the targets, the BP and WBP networks are trained.

Continuous VSP method:

(d) Selecting some parent vectors from the design variables space.
(e) Evaluating natural frequencies of the dams using trained BP and WBP networks.
(f) Evaluating the objective function.
(g) Checking the constraints for feasibility of parent vectors.
(h) Generating offspring vectors using continuous crossover and continuous mutation operators.
(i) Employing the trained BP and WBP networks for predicting the natural frequencies of the offspring population.
(j) Evaluating the objective function.
(k) Checking the constraints; if satisfied continue, else change the vector and go to step (i).
(l) Checking convergence; if satisfied stop, else go to step (i).
(m) Selecting the majority of parent vectors from the previous solution and some random design variables as a VSP.
(n) Repeating steps (f) to (m) until the proper solution is met.

As the size of populations in VSP is small the method is rapidly converged. It can be observed that during optimization process, the modal analysis of the dam- water systems is not needed.

7. NUMERICAL RESULTS

Shape optimization of double curvature arch dam with a height of 180 m is examined. The width of the valley in its bottom and top are 40 m and 220 m, respectively. In order to create the arch dam geometry, three cubic functions are considered for $t_c(z)$, $r_u(z)$ and $r_d(z)$, respectively. Therefore, by accounting two shape parameters needed to define the curve of upstream face $b(z)$, dam can be modeled by 14 shape design variables. The lower and upper bounds of design variables using empirical design methods are as:

$$
\begin{array}{llll}
0 \le s \le 0.3 & 5\text{m} \le t_{c1} \le 15\text{m} & 50\text{m} \le r_{u1} \le 160\text{m} & 50\text{m} \le r_{d1} \le 160\text{m} \\
0 < \beta \le 1 & 10\,\text{m} \le t_{c2} \le 25\,\text{m} & 40\,\text{m} \le r_{u2} \le 120\,\text{m} & 40\,\text{m} \le r_{d2} \le 120\,\text{m} \\
 & 15\,\text{m} \le t_{c3} \le 35\,\text{m} & 15\,\text{m} \le r_{u3} \le 50\,\text{m} & 15\,\text{m} \le r_{d3} \le 50\,\text{m} \\
 & 20\,\text{m} \le t_{c4} \le 45\,\text{m} & 10\,\text{m} \le r_{u4} \le 40\,\text{m} & 10\,\text{m} \le r_{d4} \le 40\,\text{m}
\end{array} \tag{7.1}
$$

For this example natural frequency constraints are imposed as:

$$
\text{fr}_1 \ge 2.54\text{Hz} \quad \text{fr}_2 \ge 2.79\text{Hz} \quad \text{fr}_3 \ge 3.27\text{Hz} \quad \text{fr}_4 \ge 3.88\text{Hz} \quad \text{fr}_5 \ge 4.54\text{Hz} \tag{7.2}
$$

The errors between exact and approximate frequencies are also calculated using the following equation:

$$
error = \left| \frac{fr_{ap} - fr_{ex}}{fr_{ex}} \right| \times 100 \tag{7.3}
$$

where fr_{ap} and fr_{ex} represent the approximate and exact frequencies, respectively.

With the mentioned conditions, the optimization is carried out by VSP employing the following methods:

(a) exact analysis (EA)
(b) approximate analysis by BP network (BP)
(c) approximate analysis by WBP network (WBP)

Optimization process is performed by a core™ 2 Duo 2GHz CPU and the time of all computations is evaluated in clock time.

7.1. Data Selection for Training the Networks

In this study, the input space consists of geometric parameters of the arch dams. The corresponding natural frequencies of the dams are considered as the target space components. A total number of 290 arch dams are randomly generated based on geometric parameters and their natural frequencies are evaluated using ANSYS. It takes about 58 minutes. From which, 229 and 61 samples are used to train and test the networks, respectively.

7.2. Training and Testing the Networks

In this study to train and test the neural networks, MATLAB [24] is utilized. The time of BP and WBP training is 0.5 min and 0.05 min, respectively. A summery of the networks performance generality in testing mode is given in Table 7.1 and Figures 2 to 6.

Table 7.1 Maximum and mean errors of BP and WBP networks in testing mode

Network	Maximum errors (%)					Mean errors (%)				
	fr_1	fr_2	fr_3	fr_4	fr_5	fr_1	fr_2	fr_3	fr_4	fr_5
BP	24.62	26.85	17.75	20.36	14.39	5.35	4.16	6.55	4.36	2.98
WBP	07.65	20.06	11.67	05.63	09.78	1.66	2.79	3.60	2.09	2.06

7.3. Results of Optimization

Optimum solutions obtained by the various methods are given in Table 7.2 As observed in this table the solutions found by VSP are more economical and the best solution is attained by VSP using WBP network.

Table 7.2 Optimum designs of the arch dam obtained by the various methods

Variable No.	EA	BP	WBP
1	0.28	0.30	0.29
2	0.98	0.99	0.99
3	6.21	5.05	5.04
4	10.17	10.00	10.20
5	33.20	19.46	20.56
6	33.51	20.20	20.57
7	145.84	145.58	123.09
8	101.68	98.77	101.56
9	46.57	48.06	45.72
10	24.94	23.50	22.22
11	145.24	137.47	121.92
12	91.38	75.74	83.43
13	45.78	44.83	45.52
14	24.56	23.42	22.10
Dam volume (m^3)	2.83×10^5	2.80×10^5	2.70×10^5
Elapsed time (min)	4200	1.02	1.02

The errors of approximate frequencies of optimum dams, predicted by BP and WBP networks, are compared in Table 7.3.

Table 7.3 Error percentage of approximate frequencies of optimum dams

Frequency No.	BP	WBP
1	1.80	1.33
2	5.76	4.63
3	8.86	3.13
4	10.2	3.94
5	4.68	4.46
Ave.	6.26	3.50

As given in this table, although the accuracy of approximate frequencies obtained by all the methods is high, the accuracy of results obtained by VSP method using WBP network is higher.

The present study demonstrates that the combination of VSP method and neural networks creates a reliable and powerful tool for optimization of arch dams including water effects with multiple natural frequency constraints.

9. CONCLUSION

An efficient optimization procedure is introduced to find the optimal shape of double curvature arch dams involving fluid-structure interaction with the frequency constraints. To achieve this aim, a finite element model based on modal analysis of arch dam-water system is presented. The results of finite element model are compared with those of reported in literature and its performance is verified. To optimize the arch dam a combination of the evolutionary algorithm and neural networks is utilized. The evolutionary algorithm used in this investigation is continuous virtual sub population (VSP) method. In order to reduce the computational cost of the optimization process the natural frequencies of the arch dams are evaluated using properly trained back propagation (BP) and wavelet back propagation (WBP) neural networks instead of their exact modal analysis. To calculate the optimal value of dilation factor of WBP neurons, a simple procedure is implemented based on estimation of performance generality of the network. The results of the networks test reveal the higher performance generality of the WBP comparing with BP networks. Numerical results also indicate that the best optimal solution is attained by VSP method using WBP network.

REFERENCES

[1] Gholizadeh, S., Salajegheh, E., and Torkzadeh, P. (2008). Structural optimization with frequency constraints by genetic algorithm using wavelet radial basis function neural network. *Journal of Sound and Vibration* **312:1-2**, 316-331.
[2] Zhu, B., Rao, B., Jia, J. and Li, Y. (1992) Shape optimization of arch dam for static and dynamic loads. *Journal of Structural Engineering, ASCE* **118:11**, 2996-3015.
[3] Zhu, B. (1987). Shape optimization of arch dams. *Water Power & Dam Construction* 43-48.
[4] Yao, T.M. and Choi, K.K. (1989). Shape optimal design of an arch dam. *Journal of Structural Engineering*, *ASCE*, **115:9**, 2401-2405.
[5] Mathias, J.D., Balandraud, X. and Grediac, M. (2006). Applying a genetic algorithm to the optimization of composite patches. *Computers & Structures* **84:12**, 823-834.
[6] Govindaraj, V. and Ramasamy, J.V. (2005). Optimum detailed design of reinforced concrete continuous beams using Genetic Algorithms. *Computers & Structures* **84:1-2**, 34-48.
[7] Madeira, J.F.A., Rodrigues, H. and Pina, H. (2005). Multi-objective optimization of structures topology by genetic algorithms. *Advances in Engineering Software* **36:1**, 21-28.
[8] Perez, R.E. and Behdinan, K. (2007). Particle swarm approach for structural optimization, *Computer & Structure* **85:19-20**, 1579-1588.
[9] Salajegheh, E. and Gholizadeh, S. (2005). Optimum design of structures by an improved genetic algorithm and neural networks. Advances in Engineering Software **36:11-12**, 757-767.
[10] Adeli, H. and Jiang, X. (2006). Dynamic fuzzy wavelet neural network model for structural system identification. *Journal of Structural Engineering, ASCE* **132:1**, 102-111.
[11] Salajegheh, E. and Heidari, A. (2005). Optimum design of structures against earthquake by wavelet neural network and filter banks. *Earthquake Engineering and Structural Dynamics* **34:1**, 67–82.
[12] Lagaros, N.D. and Papadrakakis, M. (2004). Learning improvement of neural networks used in structural optimization. *Advances in Engineering Software* **35:1**, 9-25.
[13] Fang, X., Luo, H. and Tang, J. (2005). Structural damage detection using neural network with learning rate improvement. *Computers & Structures* **83:25-26**, 2150-2161.
[14] Hall, J.F. and Chopra, A.K. (1983). Dynamic analysis of arch dams including hydrodynamic effects, *Journal of Engineering Mechanic*, *ASCE* **109:1**, 149-167.
[15] ANSYS Release 10.0 Documentation, ANSYS Incorporated, 2006.
[16] Aftabi, A. and Lotfi, V. (2007). Linear dynamic analysis of arch dams utilizing modified efficient fluid hyper-element, *Engineering Structures* **29:10**, 2654-2661.
[17] Kucukarslan, S., Coskun, B. and Taskin, B. (2005). Transient analysis of dam-reservoir interaction including the reservoir bottom effects, *Journal of Fluids and Structures* **20:8**, 1073-1084.
[18] Tan, H. and Chopra, A.K. (1996). Dam-foundation rock interaction effects in earthquake response of arch dams, *Journal of Structural Engineering*, **122:5**, 528-538.
[19] Duron, Z.H. and Hall, J.F. (1988). Experimental and finite element studies of the forced vibration response of Morrow Point dam. *Earthquake Engineering and Structural Dynamics* **16:7**, 1021-1039.
[20] Duron, Z.H. (1988). Experimental and finite element studies of a large arch dam, PhD Thesis, California Institute of Technology Pasadena, California, USA.
[21] Lekutai, G. (1997). Adaptive self-tuning neuro wavelet network controllers, Ph.D. Thesis, The Electrical Engineering Department, Virginia Polytechnic Institute and State University.
[22] Daubechies I. (1992). Ten lectures on wavelets. SIAM.
[23] Hagan, M.T. and Menhaj, M. (1999). Training feed-forward networks with the Marquardt algorithm. IEEE Transaction on Neural Networks **5:6**, 989-993.
[24]The Language of Technical Computing. MATLAB. Math Works Inc, 2006.